veterinary sciences

MDPI

Article

PRV-Induced mROS–HIF-1α Pathway-Mediated Glycolysis to Promote Replication

Qing Xu [1,2,†], Yu Wang [1,2,†], Yulin He [1,2], Zhibiao Bian [1], Pinpin Chu [1], Chunling Li [1], Shao-Lun Zhai [1], Yan Li [1], Zhiyong Jiang [1], Xia Zhou [1], Huahua Kang [1,*] and Hongchao Gou [1,*]

[1] Institute of Animal Health, Guangdong Academy of Agricultural Sciences, Guangdong Provincial Key Laboratory of Livestock Disease Prevention, Scientific Observation and Experiment Station of Veterinary Drugs and Diagnostic Techniques of Guangdong Province, Guangdong Provincial Key Laboratory of Research on the Technology of Pig-Breeding and Pig-Disease Prevention, Guangzhou 510640, China; xq238164180@163.com (Q.X.); wangyugmm@163.com (Y.W.); heyulin0813@163.com (Y.H.); m15013267255@163.com (Z.B.); cpp1900@163.com (P.C.); lclclare@163.com (C.L.); zhaishaolun@163.com (S.-L.Z.); cyhlly@126.com (Y.L.); jiangzy8839@163.com (Z.J.); xiazhou698868@163.com (X.Z.)

[2] Guangdong Laboratory for Lingnan Modern Agriculture, College of Veterinary Medicine, South China Agricultural University, Guangzhou 510642, China

* Correspondence: huahuakang2005@163.com (H.K.); gouhc@outlook.com (H.G.)

† These authors contributed equally to this work and share first authorship.

Simple Summary

Pseudorabies virus causes severe disease in pigs and can also infect humans, threatening both agriculture and public health. In this study, we investigated how PRV alters cellular glycolysis to benefit its own replication. We found that PRV activates HIF-1α and the mRNA transcription of glycolysis genes via mROS. Blocking either mROS or HIF-1α sharply reduced viral replication. These results reveal a new mechanism by which PRV rewires host glycolysis and point to potential targets for antiviral drugs, which could help control the disease in pigs and reduce the risk to human health.

Abstract

Viruses have evolved numerous mechanisms to target key metabolic pathways in the host, thereby reshaping host metabolism to establish a metabolic environment conducive to their replication. We previously observed that pseudorabies virus (PRV) infection upregulates cellular glycolysis, but the mechanism is not clear. Here, our results showed that PRV infection significantly upregulated the mRNA levels of HK2 and MCT4. Upon HIF-1α inhibition, the PRV-induced upregulation of glycolytic genes was reversed. Concurrently, PRV infection promoted the accumulation of intracellular mitochondrial ROS (mROS), whereas mROS inhibition blocked HIF-1α activation. Furthermore, both HIF-1α and mROS inhibition significantly reduced PRV replication. In conclusion, we revealed that PRV activates HIF-1α by inducing mROS accumulation, thereby upregulating key glycolytic genes to promote viral replication. This study provides novel evidence for the metabolic regulatory mechanisms underlying PRV infection and identifies potential targets for PRV and other herpesvirus control.

Keywords: pseudorabies virus (PRV); glycolysis; HIF-1α; mitochondrial ROS (mROS)

Check for updates

Academic Editors: Gang Wang and Ning Kong

Received: 30 August 2026
Revised: 13 October 2026
Accepted: 14 October 2026
Published: 23 October 2026

Copyright: © 2026 by the authors. Licensee MDPI, Basel, Switzerland. This article is an open access article distributed under the terms and conditions of the Creative Commons Attribution (CC BY) license.

1. Introduction

Pseudorabies virus (PRV), a member of the family Alphaherpesviridae, is an enveloped double-stranded DNA virus. PRV has a broad host range, including pigs, cattle, sheep, dogs, cats, mice, and rabbits, leading to pseudorabies. Pigs are the sole natural host of PRV, with susceptibility across all age groups. PRV targets the nervous, respiratory, and reproductive systems of pigs, resulting in substantial economic losses to the swine industry. In recent years, PRV has exhibited a risk of cross-species transmission, with an increasing number of reports documenting human infections [1]. Currently, vaccination remains the primary strategy for controlling pseudorabies. However, it only prevents clinical manifestations in infected pigs and fails to fully block PRV latent infection and viral shedding—posing a key challenge to the eradication of the disease in piglets. Therefore, in-depth investigations into the mechanisms underlying PRV infection and replication are warranted to provide a theoretical basis for the development of novel antiviral strategies.

As non-cellular entities, viruses are obligately dependent on energy and metabolic compounds generated by host cells to sustain their replication. The metabolic state of host cells is tightly associated with the progression of disease following viral infection. To establish a metabolic environment conducive to their replication, viruses have evolved numerous mechanisms to target key metabolic pathways in the host, thereby reshaping host metabolism to hijack metabolic resources [2]. Glycolysis is the metabolic process by which a single glucose molecule is converted into two pyruvate molecules under anaerobic conditions. In the glycolytic pathway of glucose metabolism, ten distinct metabolic enzymes act synergistically to mediate the stepwise catabolism of glucose, concomitantly generating energy stored in the form of ATP, catalyzing the conversion of nicotinamide adenine dinucleotide (NAD^+) to its reduced counterpart NADH, and yielding pyruvate. Previous studies have demonstrated that many viruses, including adenovirus, herpes simplex virus type 1 (HSV-1), and Kaposi's sarcoma-associated herpesvirus (KSHV), can reprogram cellular energy metabolism toward glycolysis to meet their replicative demands [3–5]. In our prior metabolomics analysis of PRV-infected PK-15 cells, we observed that PRV infection upregulates cellular glycolysis, but the mechanism is not clear.

Hypoxia-inducible factor-1 (HIF-1) is an oxygen-dependent heterodimeric transcription factor that plays a crucial role in a broad spectrum of physiological processes, including cardiovascular development, erythropoiesis, chondrogenesis, tumor development and progression, and metabolic regulation [6,7]. HIF-1 is a heterodimer composed of an α subunit and a β subunit, with HIF-1α serving as the primary regulator of HIF-1 activity. Under normoxic conditions, HIF-1α is hydroxylated by oxygen-dependent prolyl hydroxylases (PHDs), followed by ubiquitination and subsequent degradation via the proteasomal pathway. Under hypoxic conditions, due to reduced PHD activity, HIF-1α hydroxylation is abrogated, allowing HIF-1α to stabilize and translocate to the nucleus. Within the nucleus, HIF-1α binds to HIF-1β and the transcriptional co-activators P300/CBP, thereby driving the transcription of downstream target genes [8]. Accumulating evidence indicates that certain viral infections can enhance cellular glycolysis and remodel cellular metabolism by inducing HIF-1α activation. For example, the E6 and E7 viral oncoproteins of human papillomavirus type 16 (HPV16) induce HIF-1α activation, leading to enhanced cellular glycolysis [9]. Hepatitis C virus (HCV) stabilizes HIF-1α, upregulates key glycolytic enzymes, and suppresses the TCA cycle in infected cells [10]. Notably, a complex regulatory network exists between mitochondrial dynamics and HIF-1α, which coordinately regulates cellular biological processes. Mitochondrial dynamics can regulate HIF-1α activity by modulating the production of reactive oxygen species (ROS) [11].

This study aims to investigate the regulatory mechanism by which PRV modulates glycolysis in PK-15 cells to promote PRV replication. We found that PRV activated the

mitochondrial ROS/HIF-1α pathway and upregulated the mRNA levels of HK2 and MCT4. Thus, our study provides a novel mechanism for PRV reprogramming of glucose metabolism during replication. It is helpful for developing novel antiviral strategies for the prevention and eradication of PRV.

2. Materials and Methods

2.1. Viruses and Cells

The porcine kidney cell line PK-15 (CCL-33, ATCC) was maintained in Dulbecco's Modified Eagle Medium (DMEM; Gibco, cat. no. 11965092, Thermo Fisher Scientific, Madison, WI, USA) supplemented with 10% fetal bovine serum (FBS; Biological Industries, Kibbutz Beit Haemek, Israel) at 37 °C in a 5% CO_2 incubator. The virulent PRV GD-WH strain (GenBank accession number: KT948051) was isolated in 2015 from the brain tissue of a PRV-suspected pig, and purified virus stocks were obtained following multiple rounds of plaque purification. Porcine Nasal Mucosal Epithelial Cells (PDOT-C111, HyCyte).

2.2. Biochemical Reagents and Antibodies

BAY87-2243 (HY-100017) and Mito-Q (HY-100116A) inhibitors were purchased from MedChemExpress (Monmouth Junction, NJ, USA). The mitochondrial superoxide red fluorescent probe MitoSOX Red Mitochondrial Superoxide Indicator (40778ES50) was obtained from Beyotime Biotechnology (Shanghai, China). Primary antibodies used in this study included mouse monoclonal anti-β-Actin (AF0003, Beyotime Biotechnology, Shanghai, China) and rabbit polyclonal anti-HIF-1α (AF7087, Beyotime Biotechnology, Shanghai, China). For Western blotting, HRP-conjugated goat anti-mouse IgG (BS12478, St. Louis Park, Bioworld Technology, MN, USA) and HRP-conjugated goat anti-rabbit IgG (BS13278, Bioworld Technology, St. Louis Park, MN, USA) were used as secondary antibodies.

2.3. Virus Titer Determination

Cells were seeded in 96-well plates at a volume of 100 μL per well and incubated in a humidified 37 °C, 5% CO_2 incubator for 12–24 h until a confluent monolayer was formed. The culture medium was aspirated, and wells were rinsed once with phosphate-buffered saline (PBS) before adding an equal volume of pre-diluted virus supernatant. Serial 10-fold dilutions of the test virus supernatant were prepared in 1.5 mL centrifuge tubes, yielding eight dilution gradients (10^{-1} to 10^{-8}). The number of wells exhibiting cytopathic effects (CPE) was recorded daily until maximal CPE or cell apoptosis was observed. The 50% tissue culture infectious dose (TCID50) of the test virus was calculated using the Reed–Muench method.

2.4. Drug Inhibition Assay

Each inhibitor was pre-diluted to its working concentration in serum-free DMEM following the manufacturer's instructions. When cells reached 50–70% confluence, the original medium was aspirated, and the pre-diluted inhibitors were added. Cells were then incubated in a humidified 37 °C, 5% CO_2 incubator for 1 h. Subsequently, the inhibitor solution was removed, and cells were rinsed three times with PBS. After 30 min of viral adsorption, the virus solution was discarded, cells were rinsed three times with PBS, and the pre-diluted inhibitors were re-added.

2.5. Detection of Mitochondrial Reactive Oxygen Species (mROS)

Using a 6-well plate as an example, mROS levels were assessed using a commercial ROS detection kit following the manufacturer's protocol. The fluorescent probe MitoSOX™ was diluted 1000-fold in serum-free DMEM to a final concentration of 10 μM. Prior to

staining, the cell culture medium was aspirated, and cells were rinsed twice with PBS. Subsequently, 1 mL of the diluted MitoSOX™ working solution was added to each well, and cells were incubated in a humidified 37 °C, 5% CO_2 incubator for 20 min. After incubation, the MitoSOX™ solution was discarded, and cells were washed three times with serum-free DMEM to remove uninternalized probe. mROS production was then visualized directly under a laser scanning confocal microscope (LSCM).

2.6. Western Blotting

Cells were washed with ice-cold PBS and lysed in RIPA lysis buffer (P0013B, Beyotime) containing 1 mM PMSF (ST506, Beyotime) for 10 min on ice. Following centrifugation at 14,000× *g* for 10 min at 4 °C, the protein supernatant was collected, and protein concentration was quantified using a BCA protein assay kit (P0009, Beyotime). A 20 μg aliquot of protein was separated by 12% SDS-PAGE and electrotransferred onto a PVDF membrane (IPVH00010, Millipore, Burlington, MA, USA). The membrane was blocked in PBS containing 5% skim milk and 0.1% Tween 20 at 25 °C for 1 h and then incubated with primary antibodies at 4 °C overnight, followed by HRP-conjugated secondary antibodies at 37 °C for 1 h. Protein bands were visualized using an ECL Plus kit (P0018FS, Beyotime Biotechnology, Shanghai, China), and chemiluminescence signals were captured using a Tanon Fine-doX6 imaging system.

2.7. Quantitative Polymerase Chain Reaction (qPCR)

Total genomic DNA was isolated using the Tissue DNA Kit (D3396-02, Omega Bio-Tek/Ω, Norcross, GA, USA) according to the manufacturer's instructions. Total cellular RNA was extracted using the Total RNA Kit I (R6834-01, Omega Bio-Tek/Ω, Norcross, GA, USA). cDNA was synthesized from 1 μg of total RNA using the HiScript III RT SuperMix for qPCR (R323-01, Vazyme, Nanjing, China). The RT-qPCR primer sequences are listed in Table 1. RT-qPCR was performed using the ChamQ Universal SYBR qPCR Master Mix (Q711-02, Vazyme, Nanjing, China) on the Gentier 96R detection system (Xi'an Tianlong Science and Technology Co., Ltd., Xi'an, China).

Table 1. Primers for qPCR.

Primer Name	Title 2
Sus-Actin-qPCR-F	GGACTTCGAGCAGGAGATGG
Sus-Actin-qPCR-R	AGGAAGGAGGGCTGGAAGAG
PRV-gE-qPCR-F	ACGTTCGACCTGATGCCG
PRV-gE-qPCR-R	GGTGGTAGATGCAGGGCT
Sus-HK2-qPCR-F	CTCGCATCTGCTCGCCTACT
Sus-HK2-qPCR-R	TCCAAGCCCTTTCTCCATCT
Sus-MCT4-qPCR-F	TCATCTTCACGGTGCTCCTGG
Sus-MCT4-qPCR-R	CCTCGGGTGTCTTGTCGCTTT

2.8. Statistical Analysis

Data were analyzed using *t*-tests in GraphPad Prism V8.0 software. A p-value < 0.05 denoted a significant difference.

2.9. Cell Viability Assay

Cell viability was measured using a Cell Counting Kit-8 (CCK-8) assay kit (C0037, Beyotime) according to the manufacturer's instructions. Briefly, PK-15 cells were cultured in 96-well culture plates at a seeding density of 1×10^4 cells per well for 24 h. Then, the medium was replaced with 100 μL of DMEM containing one of the following inhibitors:

200 nM BAY87 or 2 μM Mito-Q. After 12 h, cells were washed three times with PBS and cultured in 100 μL of DMEM containing 10 μL of CCK-8 for 1 h at 37 °C. The optical density was measured at 450 nm using a microplate reader.

2.10. Language Editing

The DeepSeek software (DeepSeek-V4.1-Flash https://www.deepseek.com/) was used for language editing to improve the writing quality.

3. Results

3.1. PRV Infection Upregulates the Transcriptional Levels of Key Glycolytic Genes

Our previous metabolomic analysis of PRV-infected PK-15 cells revealed that PRV infection enhances cellular glycolysis [12]. To further investigate the specific mechanisms by which PRV remodels cellular glycolysis, we measured the mRNA transcription levels of two key glycolytic enzymes, hexokinase 2 (HK2) and monocarboxylate transporter 4 (MCT4), in PRV-infected PK-15 cells at 4, 8, and 12 h. qPCR results demonstrated that PRV infection significantly upregulated the mRNA expression of HK2 and MCT4 in PK-15 cells at all tested time points (Figure 1).

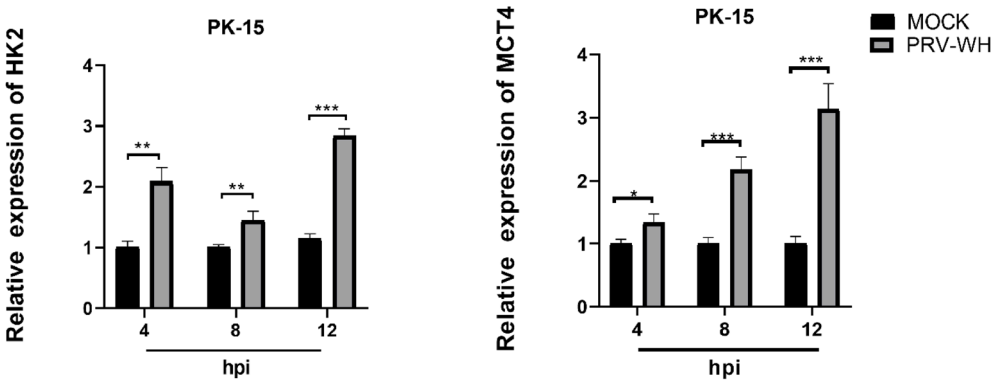

Figure 1. PRV infection upregulates the transcriptional levels of key glycolytic genes in PK-15 cells. PK-15 cells were infected with PRV (MOI = 1) for 4, 8, and 12 h. RT-qPCR was then performed to examine the mRNA expression levels of HK2 and MCT4, two critical regulators of glycolysis, at the indicated time points. Asterisks indicate significant differences compared with the MOCK group (* $p < 0.05$, ** $p < 0.01$, *** $p < 0.001$).

3.2. PRV Activates HIF-1α to Promote the Expression of Key Glycolytic Genes

HIF-1α plays a critical role in the remodeling of host cell glycolysis following viral infection. To determine whether PRV-induced glycolytic enhancement is HIF-1α-dependent, PK-15 cells were pretreated with the HIF-1α-specific inhibitor BAY87-2243 (200 nM) prior to PRV infection. qPCR was then used to assess the mRNA expression levels of MCT4 and HK2. The results demonstrated that PRV infection induced HIF-1α activation, and this activation was abrogated by BAY87-2243 pretreatment (Figures 2a, S1 and S2). Furthermore, inhibition of HIF-1α activation significantly attenuated PRV-induced upregulation of HK2 and MCT4 mRNA expression (Figure 2b).

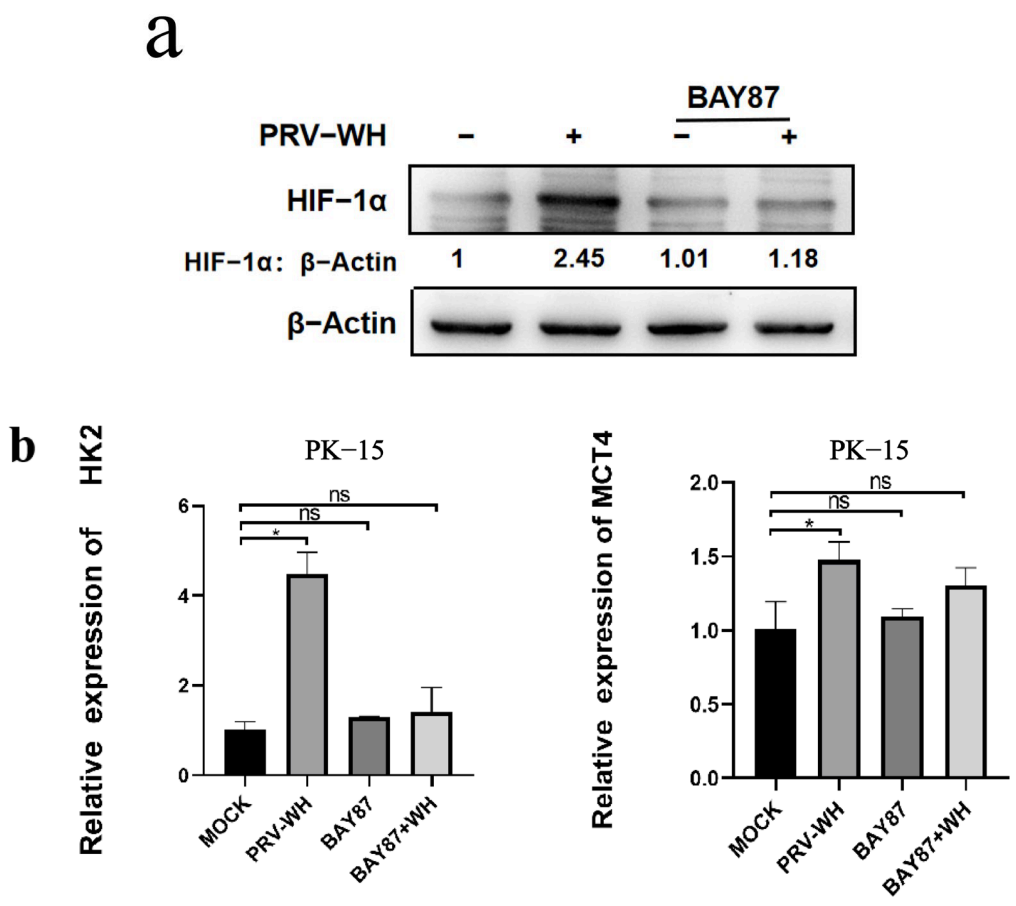

Figure 2. PRV activates HIF-1α to promote glycolysis in PK-15 cells: (**a**,**b**) PK-15 cells were divided into four experimental groups: mock-infected control, PRV-WH infection alone, BAY87 (200 nM) treatment alone, and PRV-WH infection combined with BAY87 pretreatment. Cells were pretreated with BAY87 for 1 h, followed by infection with PRV-WH (MOI = 1). (**a**) Western blot analysis was performed to examine the protein expression level of HIF-1α in each group, with β-actin used as the loading control. (**b**) RT-qPCR was employed to determine the mRNA expression levels of HK2 and MCT4 in each group (* $p < 0.05$, "ns" indicates no significant difference).

3.3. PRV-Induced HIF-1α Activation Is Dependent on mROS Production

ROS are major inducers of HIF-1α, and cellular ROS primarily originate from dysfunctional mitochondria [11]. To investigate whether mROS are involved in HIF-1α activation, we first assessed mROS levels in PK-15 cells following PRV infection. The results demonstrated that PRV infection significantly induced mROS production (Figures 3a and S3–S8). Next, we pretreated PK-15 cells with the mROS-specific inhibitor Mito-Q (2 μM) prior to PRV infection. Inhibition of mROS production abrogated PRV-induced HIF-1α activation (Figures 3b, S9 and S10), indicating that PRV-mediated HIF-1α activation is dependent on mROS generation. Furthermore, PRV infection also induced mROS production in porcine nasal mucosal epithelial cells (Figures 3c and S11–S16), indicating that PRV-induced mROS generation is not restricted to the immortalized PK-15 cell line.

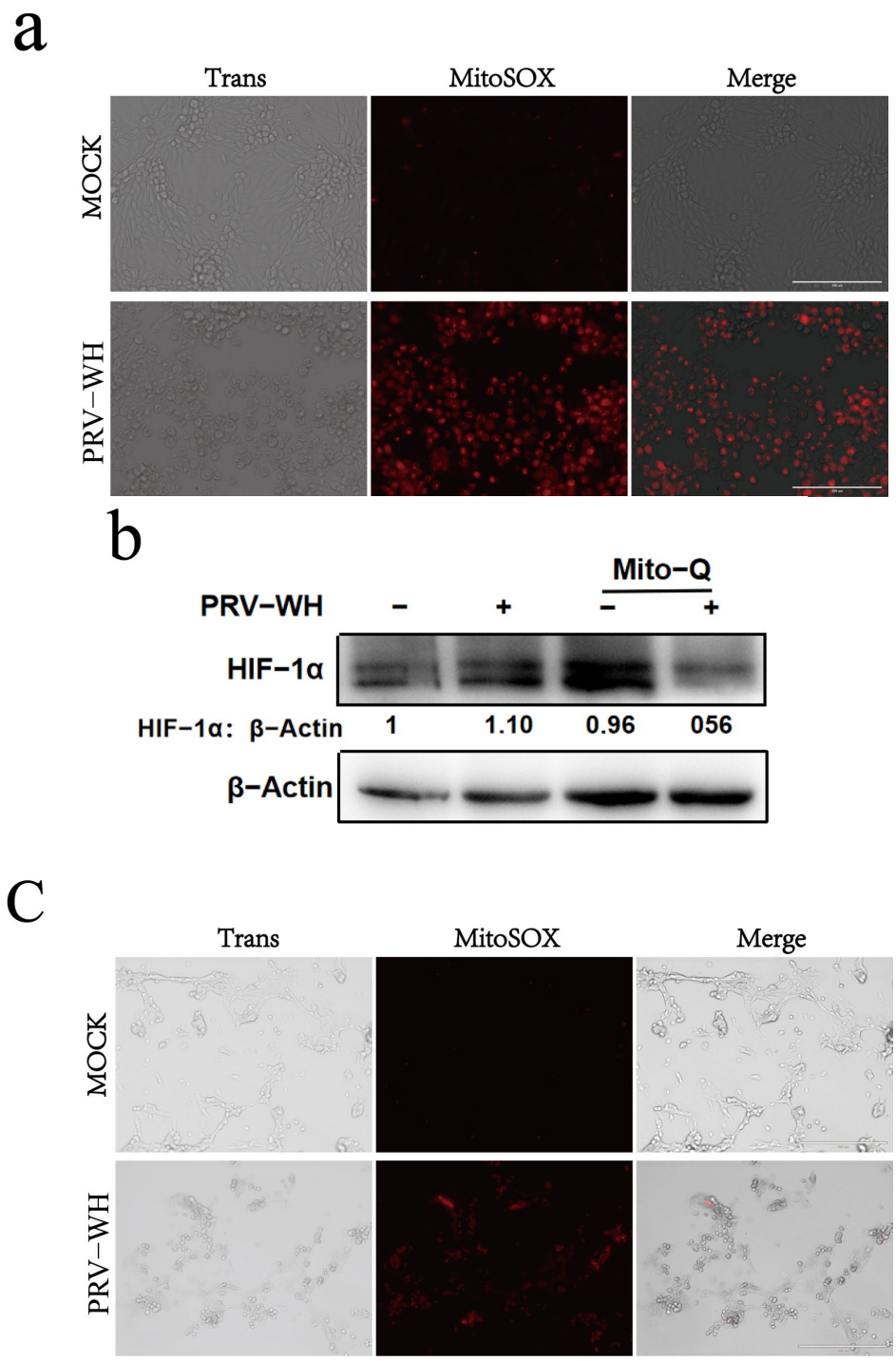

Figure 3. PRV-induced HIF-1α activation is dependent on mROS generation in PK-15 cells. (**a**) PK-15 cells were mock-infected or infected with PRV-WH (MOI = 1). Cells were incubated with MitoSOX (10 μM) in serum-free DMEM at 37 °C for 20 min, followed by three washes with serum-free DMEM. mROS production was then visualized under a laser scanning confocal microscope. (**b**) PK-15 cells were divided into four experimental groups: mock-infected control, Mito-Q (2 μM) treatment alone, PRV-WH infection alone, and PRV-WH infection combined with Mito-Q pretreatment. Cells were pretreated with Mito-Q for 1 h, followed by infection with PRV-WH (MOI = 1). Western blot analysis was performed to examine the protein expression level of HIF-1α in each group, with β-actin used as the loading control. (**c**) PRV Infection Induces mROS Production in Porcine Nasal Mucosal Epithelial Cells. Cells were mock-infected or infected with PRV-WH, and mROS levels were assessed at 12 h post-infection using MitoSOX (10 μM) under an inverted fluorescence microscope. Representative images of the TRANS and RFP channels are shown.

3.4. Inhibition of mROS Generation or HIF-1α Activity Attenuates PRV Replication

To investigate whether HIF-1α plays a role in regulating PRV replication, PK-15 cells were pretreated with BAY87 prior to PRV infection. The relative intracellular DNA levels of the PRV gE gene upon BAY87 treatment were analyzed by qPCR. Meanwhile, viral supernatants were collected for TCID50 assays. The results showed that inhibiting HIF-1α activation reduced both the intracellular DNA levels of the PRV gE gene and viral titers of cell supernatants, indicating that HIF-1α activation is necessary for PRV replication (Figure 4a). Furthermore, PK-15 cells were pretreated with the mROS inhibitor Mito-Q (2 μM) prior to PRV infection. The results indicated that when mROS production was inhibited, both the relative intracellular DNA levels of the PRV gE gene and viral titers of cell supernatants were reduced (Figure 4b). In addition, the CCK-8 assay showed that cell viability remained above 80% in both BAY87-2243 (200 nM) and Mito-Q (2 μM) treated groups (Figure 4c), excluding the possibility that the reduced viral replication was due to non-specific cytotoxicity.

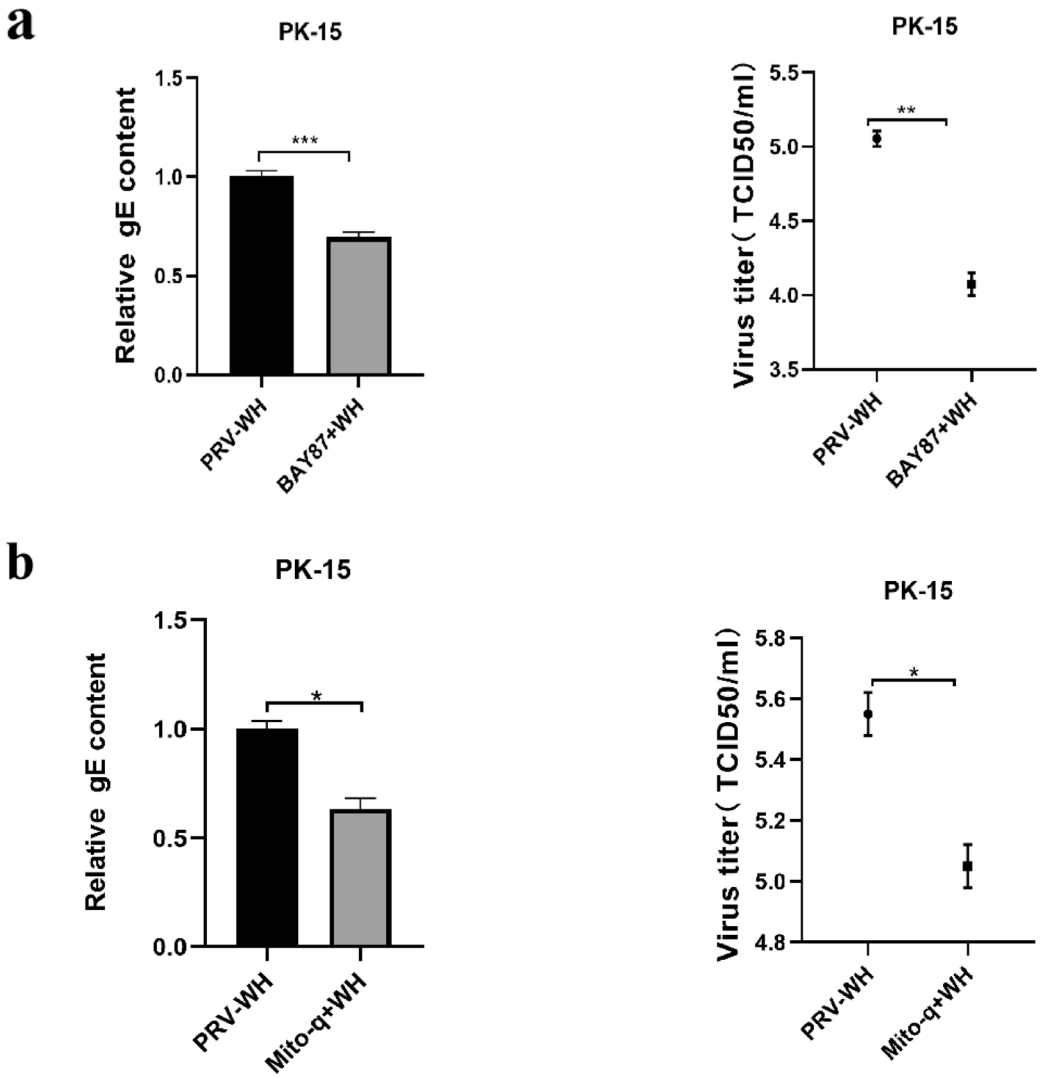

Figure 4. *Cont.*

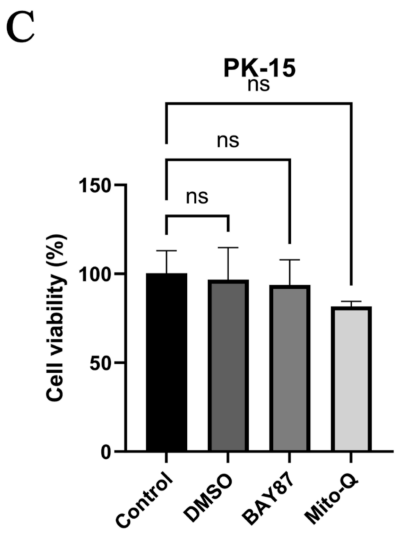

Figure 4. Inhibition of mROS generation or HIF-1α activity attenuates PRV replication capacity in PK-15 cells: (**a**,**b**) PK-15 cells were divided into two groups: PRV-WH infection alone and PRV-WH infection combined with inhibitor pretreatment. Cells were pretreated with the respective inhibitor for 1 h, followed by infection with PRV-WH (MOI = 1). The intracellular PRV genomic DNA level was determined by quantifying the gE gene via qPCR normalized to β-actin (left panels), and viral titers in the culture supernatants were measured using the $TCID_{50}$ assay (right panels). (**a**) Cells were pretreated with BAY87 (200 nM). (**b**) Cells were pretreated with Mito-Q (2 μM). (**c**) Cytotoxicity assessment of BAY87-2243 and Mito-Q in PK-15 cells. Cells were pretreated with BAY87-2243 (200 nM) or Mito-Q (2 μM) for 1 h, and cell viability was determined by CCK-8 assay. Relative cell viability was calculated with the untreated group set as 100%. Data are presented as mean ± SD. (* $p < 0.05$, ** $p < 0.01$, *** $p < 0.001$, "ns" indicates no significant difference).

4. Discussion

PRV inflicts substantial economic losses on the global swine industry, and emerging reports of human infections have raised concerns about its potential threat to public health. The characteristics of latent infection and intermittent viral shedding in pig herds pose significant challenges to the eradication of PRV. Therefore, a thorough understanding of the mechanisms underlying PRV infection and replication is critical for the development of novel prevention and control strategies. In this study, we found that PRV induced mitochondrial ROS production and subsequent activation of the downstream HIF-1α pathway, which ultimately drives glycolytic activation by upregulating the mRNA transcription levels of HK2 and MCT4 (Figure 5).

As a class of acellular obligate intracellular parasites, viruses are entirely dependent on host-derived macromolecules for their assembly and replication. To hijack metabolic resources, viruses have evolved diverse strategies to manipulate host metabolism by targeting key metabolic pathways. Virally infected cells typically exhibit the Warburg effect, also termed aerobic glycolysis, whereby glycolytic flux is upregulated even under oxygen-replete conditions, thereby providing reducing equivalents and biosynthetic precursors to support macromolecular biosynthesis [13]. Building on our prior work demonstrating that PRV upregulates glycolytic flux in PK-15 cells [12], this study further analyzed the transcriptional dynamics of key glycolytic genes. Our results revealed that PRV induces HIF-1α activation to upregulate the mRNA transcription levels of HK2 and MCT4. However, relying solely on HK2 and MCT4 mRNA levels, without direct functional validation of metabolic flux, is a limitation of the present study. Accumulating evidence indicates that multiple viruses promote glycolysis via HIF-1α-mediated regulation. For example, respiratory syncytial virus (RSV) infection upregulates both glycolytic flux and pentose phosphate pathway (PPP)

activity. When HIF-1α is inhibited, the expression of HK2 and pyruvate dehydrogenase kinase 1 (PDK1) decreases, concomitant with suppressed viral replication [14]. Consistently, our study demonstrated that inhibition of HIF-1α activation via BAY87 treatment significantly impaired PRV replication in vitro, indicating a tight correlation between HIF-1α-dependent glycolytic upregulation and PRV propagation. Similarly, studies on KSHV have confirmed that HIF-1α expression under normoxic conditions markedly enhances lytic gene expression during de novo infection [15]. However, metabolic requirements vary among herpesviruses. For instance, HSV-1 replication relies more on the diversion of glucose metabolism toward nucleotide biosynthesis [16], whereas PRV propagation is more dependent on glycolytic enhancement.

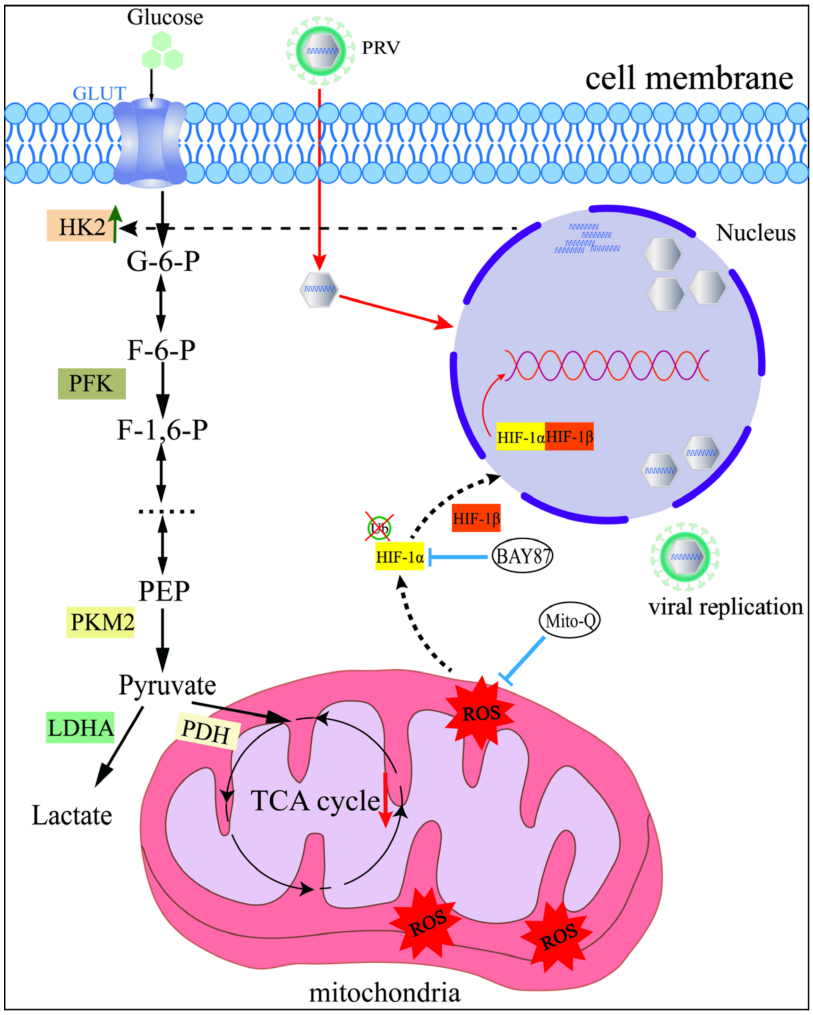

Figure 5. Mechanism diagram of the PRV-induced mROS–HIF-1α pathway-mediated glycolysis to promote replication.

Furthermore, accumulating evidence highlights that ROS are critical for maintaining HIF-1α stability and activation [17]. Mitochondria serve as the primary source of ROS in eukaryotic cells, and mitochondrial damage triggered by environmental stress or pathogen-induced stimuli can lead to a surge in intracellular ROS levels in host cells. Our study revealed that PRV infection induces mROS production. Inhibition of mROS generation attenuated HIF-1α activation and PRV replication. Similar observations have been reported in other viruses. For example, SARS-CoV-2 ORF3a protein elevates HIF-1α levels by impairing mitochondrial function and inducing mitochondrial ROS (Mito-ROS), thereby promoting viral replication and exacerbating inflammation [18]. A significant correlation between

elevated ROS levels and influenza A virus WSN strain infection was also established [19]. Drawing upon studies on mitochondrial targeting in alphaherpesviruses, we propose that the N-terminally truncated isoform of PRV UL12 (UL12.5) represents the most plausible candidate mediator. In HSV-1, the deletion of the N-terminal nuclear localization signal in UL12.5 unmasks a mitochondrial matrix-targeting sequence, enabling its translocation to mitochondria where it degrades mtDNA [20,21]. This process disrupts oxidative phosphorylation, leading to electron leakage and subsequent ROS accumulation. Given the high conservation between PRV UL12 and its HSV-1 homolog [22] and the established observation that PRV infection induces mitochondrial morphological aberrations and membrane potential dissipation [23], we hypothesize that UL12.5-mediated mitochondrial damage constitutes an upstream event driving mROS surge.

In conclusion, this study demonstrates that PRV induces mitochondrial ROS production and subsequent activation of the downstream HIF-1α pathway, thereby upregulating mRNA levels of glycolytic enzymes HK2 and MCT4 in glycolysis in host cells. By providing novel insights into the molecular mechanisms underlying PRV-mediated metabolic reprogramming for enhanced replication, this study not only facilitates the identification of potential antiviral targets but also offers a theoretical framework for research on other herpesviruses.

Supplementary Materials: The following supporting information can be downloaded at https://www.mdpi.com/article/10.3390/vetsci13111131/s1, Figures S1 and S2: Original Western blot image for Figure 2a; Figures S3–S8: Original Western blot image for Figure 3a; Figures S9 and S10: Original Western blot image for Figure 3b; Figures S11–S16: Original Western blot image for Figure 3c.

Author Contributions: Conceptualization, H.K. and H.G.; methodology, Y.H.; software, Z.B., P.C. and S.-L.Z.; validation, C.L., Y.L. and Z.J.; formal analysis, Q.X. and Y.W.; investigation, Q.X. and Y.W.; resources, X.Z. and H.G.; data curation, Q.X. and Y.W.; writing—original draft preparation, Q.X. and Y.W.; writing—review and editing, H.K. and H.G.; visualization, Y.H.; supervision, H.K. and H.G.; project administration, H.K. and H.G.; funding acquisition, H.G. and H.K. All authors have read and agreed to the published version of the manuscript.

Funding: This work was supported by grants from the Natural Science Foundation of Guangdong, China (2024A1515030253 and 2024A1515140152), the Opening Project of the State Key Laboratory of Swine and Poultry Breeding Industry (ZQQZ-G18 and 2023QZ-NK05), the Special Funding for the Construction of the High-Level Academy of Agricultural Sciences (NYQS202615), the Key Project of Guangzhou Science and Technology Plan (2025B01J0001), and 2026 Provincial Rural Revitalization Strategy Special Project (2026CXTD 15-02).

Institutional Review Board Statement: Not applicable.

Informed Consent Statement: Not applicable.

Data Availability Statement: The original contributions presented in this study are included in the article. Further inquiries can be directed to the corresponding authors.

Acknowledgments: During the writing of this manuscript, the DeepSeek software (DeepSeek-V4.1-Flash https://www.deepseek.com/) was used for language editing.

Conflicts of Interest: The authors declare no conflicts of interest.

References

1. Ketusing, N.; Reeves, A.; Portacci, K.; Yano, T.; Olea-Popelka, F.; Keefe, T.; Salman, M. Evaluation of strategies for the eradication of pseudorabies virus (aujeszky's disease) in commercial swine farms in Chiang-Mai and Lampoon provinces, Thailand, using a simulation disease spread model. *Transbound. Emerg. Dis.* **2014**, *61*, 169–176. [CrossRef]
2. Shehata, H.M.; Murphy, A.J.; Lee, M.K.S.; Gardiner, C.M.; Crowe, S.M.; Sanjabi, S.; Finlay, D.K.; Palmer, C.S. Sugar or fat?-metabolic requirements for immunity to viral infections. *Front. Immunol.* **2017**, *8*, 1311. [CrossRef]

3. Wang, Z.Q.; Cefalu, W.T.; Zhang, X.H.; Yu, Y.; Qin, J.; Son, L.; Rogers, P.M.; Mashtalir, N.; Bordelon, J.R.; Ye, J.; et al. Human adenovirus type 36 enhances glucose uptake in diabetic and nondiabetic human skeletal muscle cells independent of insulin signaling. *Diabetes* **2008**, *57*, 1805–1813. [CrossRef]
4. Abrantes, J.L.; Alves, C.M.; Costa, J.; Almeida, F.C.; Sola-Penna, M.; Fontes, C.F.; Souza, T.M. Herpes simplex type 1 activates glycolysis through engagement of the enzyme 6-phosphofructo-1-kinase (pfk-1). *Biochim. Biophys. Acta* **2012**, *1822*, 1198–1206. [CrossRef]
5. Delgado, T.; Carroll, P.A.; Punjabi, A.S.; Margineantu, D.; Hockenbery, D.M.; Lagunoff, M. Induction of the warburg effect by kaposi's sarcoma herpesvirus is required for the maintenance of latently infected endothelial cells. *Proc. Natl. Acad. Sci. USA* **2010**, *107*, 10696–10701. [CrossRef]
6. Compernolle, V.; Brusselmans, K.; Franco, D.; Moorman, A.; Dewerchin, M.; Collen, D.; Carmeliet, P. Cardia bifida, defective heart development and abnormal neural crest migration in embryos lacking hypoxia-inducible factor-1alpha. *Cardiovasc. Res.* **2003**, *60*, 569–579. [CrossRef]
7. Yang, C.; Zhong, Z.F.; Wang, S.P.; Vong, C.T.; Yu, B.; Wang, Y.T. Hif-1: Structure, biology and natural modulators. *Chin. J. Nat. Med.* **2021**, *19*, 521–527. [CrossRef]
8. Triner, D.; Shah, Y.M. Hypoxia-inducible factors: A central link between inflammation and cancer. *J. Clin. Investig.* **2016**, *126*, 3689–3698. [CrossRef]
9. Guo, Y.; Meng, X.; Ma, J.; Zheng, Y.; Wang, Q.; Wang, Y.; Shang, H. Human papillomavirus 16 e6 contributes hif-1α induced warburg effect by attenuating the vhl-hif-1α interaction. *Int. J. Mol. Sci.* **2014**, *15*, 7974–7986. [CrossRef]
10. Ripoli, M.; D'Aprile, A.; Quarato, G.; Sarasin-Filipowicz, M.; Gouttenoire, J.; Scrima, R.; Cela, O.; Boffoli, D.; Heim, M.H.; Moradpour, D.; et al. Hepatitis c virus-linked mitochondrial dysfunction promotes hypoxia-inducible factor 1 alpha-mediated glycolytic adaptation. *J. Virol.* **2010**, *84*, 647–660. [CrossRef]
11. Belaidi, E.; Morand, J.; Gras, E.; Pépin, J.L.; Godin-Ribuot, D. Targeting the ros-hif-1-endothelin axis as a therapeutic approach for the treatment of obstructive sleep apnea-related cardiovascular complications. *Pharmacol. Ther.* **2016**, *168*, 1–11. [CrossRef]
12. Gou, H.; Bian, Z.; Li, Y.; Cai, R.; Jiang, Z.; Song, S.; Zhang, K.; Chu, P.; Yang, D.; Li, C. Metabolomics exploration of pseudorabies virus reprogramming metabolic profiles of pk-15 cells to enhance viral replication. *Front. Cell. Infect. Microbiol.* **2020**, *10*, 599087. [CrossRef]
13. Thaker, S.K.; Ch'ng, J.; Christofk, H.R. Viral hijacking of cellular metabolism. *BMC Biol.* **2019**, *17*, 59. [CrossRef]
14. Morris, D.R.; Qu, Y.; Agrawal, A.; Garofalo, R.P.; Casola, A. Hif-1α modulates core metabolism and virus replication in primary airway epithelial cells infected with respiratory syncytial virus. *Viruses* **2020**, *12*, 1088. [CrossRef]
15. Lee, S.C.; Naik, N.G.; Tombácz, D.; Gulyás, G.; Kakuk, B.; Boldogkői, Z.; Hall, K.; Papp, B.; Boulant, S.; Toth, Z. Hypoxia and hif-1α promote lytic de novo kshv infection. *J. Virol.* **2023**, *97*, e00972-23. [CrossRef]
16. Vastag, L.; Koyuncu, E.; Grady, S.L.; Shenk, T.E.; Rabinowitz, J.D. Divergent effects of human cytomegalovirus and herpes simplex virus-1 on cellular metabolism. *PLoS Pathog.* **2011**, *7*, e1002124. [CrossRef]
17. Wang, R.; Zhu, Y.; Lin, X.; Ren, C.; Zhao, J.; Wang, F.; Gao, X.; Xiao, R.; Zhao, L.; Chen, H.; et al. Influenza m2 protein regulates mavs-mediated signaling pathway through interacting with mavs and increasing ros production. *Autophagy* **2019**, *15*, 1163–1181. [CrossRef]
18. Tian, M.; Liu, W.; Li, X.; Zhao, P.; Shereen, M.A.; Zhu, C.; Huang, S.; Liu, S.; Yu, X.; Yue, M.; et al. Hif-1α promotes sars-cov-2 infection and aggravates inflammatory responses to COVID-19. *Signal Transduct. Target. Ther.* **2021**, *6*, 308. [CrossRef]
19. Zhang, Y.; Chang, L.; Xin, X.; Qiao, Y.; Qiao, W.; Ping, J.; Xia, J.; Su, J. Influenza a virus-induced glycolysis facilitates virus replication by activating ros/hif-1α pathway. *Free Radic. Biol. Med.* **2024**, *225*, 910–924. [CrossRef]
20. Saffran, H.A.; Pare, J.M.; Corcoran, J.A.; Weller, S.K.; Smiley, J.R. Herpes simplex virus eliminates host mitochondrial DNA. *EMBO Rep.* **2007**, *8*, 188–193. [CrossRef]
21. Corcoran, J.A.; Saffran, H.A.; Duguay, B.A.; Smiley, J.R. Herpes simplex virus ul12.5 targets mitochondria through a mitochondrial localization sequence proximal to the n terminus. *J. Virol.* **2009**, *83*, 2601–2610. [CrossRef]
22. Hsiang, C.Y.; Ho, T.Y.; Chang, T.J. Identification of a pseudorabies virus ul12 (deoxyribonuclease) gene. *Gene* **1996**, *177*, 109–113. [CrossRef]
23. Zhao, Y.; Ding, C.; Zhu, Z.; Wang, W.; Wen, W.; Favoreel, H.W.; Li, X. Pseudorabies virus infection triggers mitophagy to dampen the interferon response and promote viral replication. *J. Virol.* **2024**, *98*, e01048-24. [CrossRef]

Disclaimer/Publisher's Note: The statements, opinions and data contained in all publications are solely those of the individual author(s) and contributor(s) and not of MDPI and/or the editor(s). MDPI and/or the editor(s) disclaim responsibility for any injury to people or property resulting from any ideas, methods, instructions or products referred to in the content.